Catalytic Partial Oxidation of Methane to Methanol under Various Reaction Conditions

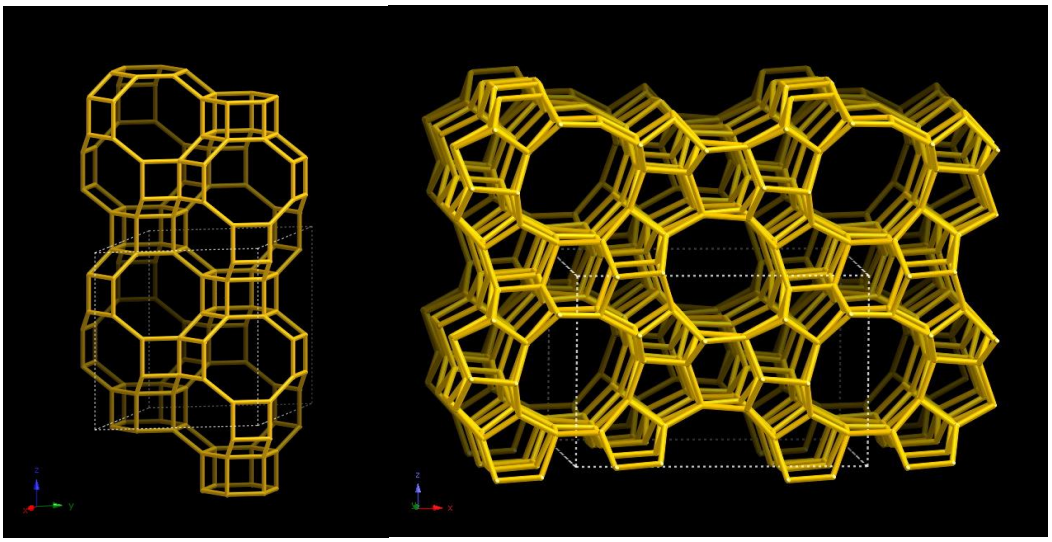

Fredrik Carlsson
Master Thesis in Chemistry and Chemical Engineering, KBTX12

Abstract

Methane is used as an energy source, a chemical feedstock and is the main constituent of natural gas. Today when natural gas is encountered while drilling for oil the gas is often flared. A process where the gas is combusted on-site. This is performed as the gas cannot be feasibly stored and transported. As methane is a potent greenhouse gas it is the preferable option to flare it rather than simply venting it.

The development of catalyst for a direct conversion of methane to methanol (DCMM) hopes to reduce the practice of flaring. Which serves to both limit the greenhouse gas emissions of the oil industry and provide a product. Copper exchanged zeolites are promising catalysts for the DCMM reaction. The methane is converted into methanol in a quasicatalytical, stepwise cycle. Where the catalyst is first activated with oxygen at high temperatures. Followed by adsorption of methane and finally extraction using water.

The DCMM reaction with copper exchanged ZSM-5 and SSZ-13 zeolites was examined under various reaction conditions in a flow reactor. Low temperature extraction (LTE) at 50^{o}C was tested and several reaction conditions where the zeolite was exposed to ammonia. In an attempt to disperse the copper in the zeolites and increasing the number of active sites. How the ammonia affected the catalysts was examined using DRIFTS.

LTE proved to be possible for both catalysts. The LTE also produced more methanol for the Cu-ZSM-5 catalyst with a higher selectivity. However, these results are questionable as the manner in which the reaction conditions were examined increases the efficiency of the catalysts. The reaction conditions using ammonia produced no methanol for the Cu-ZSM-5 catalyst. The Cu-SSZ-13 catalyst produced methanol under an isothermal, stepwise reaction cycle at 250^{o}C. Less methanol was produced than for the standard reaction conditions used. DRIFTS showed that copper-ammonia complexes form on the zeolites. Which could indicate that the compound responsible for the dispersal is present. Unfortunately, this could not be verified. No methoxy-groups were forming on the catalysts using the ammonia reaction conditions, however. Excluding the possibility that the extraction steps were failing.

Keywords: Direct conversion of methane to methanol, DCMM, Copper zeolites, Cu-ZSM-5, Cu-SSZ-13, ammonia

Table of Contents

1. Introduction 4
1.2 Aim of the Project 5
2. Background 5
2.1 Direct Conversion of Methane to Methanol 5
2.2 Zeolites 6
2.3 DCMM Over Copper Exchanged Zeolites 6
3. Experimental Methods 7
3.1 Sample Preparation 7
3.1.1 Aqueous Ion Exchange 7
3.1.2 Wash Coating 7
3.2 Nitrogen Physisorption - BET 8
3.3 X-Ray Diffraction - XRD 9
3.4 Mass Spectrometry 9
3.5 Infrared Spectroscopy 9
3.5.1 Diffuse Reflectance Infrared Fourier-Transform Spectroscopy 10
3.6 Flow Reactor 10
3.6.1 Reaction Conditions 11
4. Results 13
4.1 Flow Reactor 13
4.2 Diffuse Reflectance Infrared Fourier-Transform Spectroscopy 15
4.3 Nitrogen Physisorption - BET 19
4.4 XRD 19
5. Discussion 20
6. Conclusions 22
7. References 23

1. Introduction

Methane is a common and naturally occurring compound. It is produced by anaerobic decomposition of biological matter. It is therefore commonly, and naturally, encountered in wetlands, swamps and the bowels of cattle. Methane is also found in natural deposits, in what is referred to as natural gas. A mixture mainly composed of methane with some heavier hydrocarbons (C_{2+}), N_2 and H_2S gas. The actual composition of natural gas varies depending on the type of deposit [1].

Methane is often used as an energy source, as its composition of one carbon and four hydrogen atoms makes its combustion very energy efficient. About 23.4% of the world's energy demand is met by natural gas [2]. Which is preferable, as under complete combustion it can also be considered amongst the greenest alternatives, especially when compared to the burning of coal or oils. The low content of nitrogen and Sulphur in natural gas contributes less to acidic rain and over-fertilization [1]. However, methane gas has a considerably high global warming potential of 56 over a 20-year period [3]. Apart from being an excellent energy source, methane is used to produce synthetic gas (syngas), CO/H_2, which in turn is converted into heavier synthetic fuels, methanol or purified into pure hydrogen gas.

While natural gas can be considered a greener alternative to coal and oil. It is still a fossil fuel. Methane can be produced by renewable methods [1], making it a potential renewable and green energy source. Theoretically it is possible to produce a zero-emission cycle with methane gas. As the carbon dioxide released through burning is absorbed by growing plant matter, which in turn is used to create methane, ad infinitum. Yet this raises ethical concerns as the farmland used to produce the plant matter required might as well go to the production of food. As per 2018, 3680.4 billion m^3 of natural gas was produced worldwide, with a 4% annual growth estimate [2]. This number does not include the volume of natural gas going to waste through flaring. A process where the natural gas found and pumped up along raw oil is burned. Flaring is necessitated by the difficulties with capturing, storing and transporting natural gas. As natural gas is a profitable resource it is rarely burned simply because it is not wanted. Rather, the infrastructure capabilities in the region are unable to handle the gas, or the quantities of it. It may then be decided that expansion or development of such an infrastructure is too expensive with respect to the gas. Leading to the gas being burned. There are however practical reasons for flaring, for example sudden spikes in pressure where gas needs to be vented, during exploration of oil fields and such. Despite this, flaring of natural gas at oil wells is a considerable environmental issue. It releases pollutants and greenhouse gases for absolutely no gain. Approximately 150 billion m^3 of natural gas is flared per year around the world [4].

Transportation of methane gas is primarily conducted through pipelines or in a liquified form. Pipelines are not infallible as lack of maintenance leads to wear and tear as well as leakage of gas [5]. Another mean of transportation is to first convert the natural gas into what is simply referred to as Liquified natural gas (LNG). This is a resource intensive means of transportation, usually performed when transporting natural gas overseas. The gas is compressed and cooled to a liquid state; this requires specialized transport vehicles apart from a specialized facility for the liquefaction [5].

The difficulties with transporting natural gas prompt the question of if anything can be done on-site with the natural gas. An oil platform at sea cannot utilize a pipeline for example. Neither is it feasible to construct pipelines to remotely located oil wells. The previously mentioned syngas requires dedicated plants, and without subsequent steps to either methanol, hydrogen or synthetic fuels does not solve the issue.

A proposed solution is the development of catalysts for the partial oxidation of methane to methanol. While this does not preserve the natural gas, methanol can on its own be used as an energy source. Methanol is also used as a feedstock in the chemical industry, apart from as a direct product. Methanol is also a liquid, as such both storing and transporting is far easier than with natural gas. Most importantly, in cases where the natural gas cannot be stored or transported efficiently it would not be flared, or flared to a lesser degree, with such a system in place.

1.2 Aim of the Project

The aim is to examine different reaction conditions for the partial oxidation of methane to methanol using copper exchanged ZSM-5 and SSZ-13 zeolites.

2. Background

These sections aim to provide an insight into the direct conversion of methane to methanol reaction and the work that have been made to achieve it.

2.1 Direct Conversion of Methane to Methanol

Methane is one of the most stable molecules in existence, reactions are however not improbable. It is after all a fuel and combustion is one of the dangers when transporting it. Combustion is however the complete oxidation of methane, while conversion to methanol is partial. The issue is then not only how to initiate the reaction to methanol, but also how to inhibit further reactions to carbon dioxide [6,7,8,9]. Observing the dissociation energies associated with C-H bonds in methanol and methane illustrates the disparity to a degree. Methane has a C-H bond dissociation energy of 440 kJ/mol while in methanol it is 393 kJ/mol [6].

Research on direct conversion of methane to methanol (DCMM) began in the early 1900s. With the oxidation of methane to methanol with hydrogen peroxide, in the presence of ferrous sulfate [6]. The early 20th century was then focused on achieving DCMM utilizing iron sulfates or oxides. The yields remained low with both low conversion and selectivity [6]. The first uses of catalysts in DCMM began thereafter [6]. Initially, homogeneous catalysts were the focus for DCMM. Organometallic compounds of platinum, mercury and palladium were tested in solution with sulfuric acid. Yet these reactions were still hampered by low yields of methanol [6]. It was determined that in order to reach high selectivity of methanol in homogenous systems protection was required. The methanol was being completely oxidized otherwise. The fact that the products were highly diluted derivatives of methanol, in strong acids, made the processes unattractive for industrial applications [6]. As homogeneous catalysts saw increasingly successful results, some focus shifted towards developing heterogeneous catalysts with similar active species [6]. Iron, copper and molybdenum-based catalysts were the focus for heterogeneous catalysts [6].

During the early 2000s it was found that zeolites could stabilize copper and iron in a manner resembling those of naturally occurring enzymes, monooxygenase (MMO). These enzymes are capable of methanol production under ambient conditions and are found in bacteria [6]. This discovery promoted a shift in focus towards zeolite-based systems with copper or iron as the active species. The DCMM reaction with both copper- and iron-zeolites is quasicatalytical. It is performed in a stepwise cycle of activation, reaction and extraction. Activation can be performed with oxygen at

high temperatures. The copper zeolites typically do not require as high temperatures as the iron zeolite catalyst at this step. Since the yields of both catalysts is comparable this makes copper the more lucrative alternative [6].

2.2 Zeolites

By loose definition zeolites are minerals composed of a silicon and aluminum framework, with a tetrahedral framework structure that allows for the movement of ions and other molecules [10]. The properties of zeolites change depending on how they are synthesized, yet they can retain the same structural framework. For example, the ratios of silica and alumina may vary but the framework structure can be the same [10].

The two zeolites used in this thesis are ZSM-5 and SSZ-13. The respective framework type of the zeolites are MFI and CHA, chabazite. The structural framework of both zeolites is shown in figure 1. ZSM-5 possesses straight channels of 10-membered rings, as well as smaller, parallel channels of 6-, 5- and 4-membered rings [11]. SSZ-13 is however built up by a framework of cages, as opposed to straight channels. The openings to these cages are 6- and 8-membered rings [12].

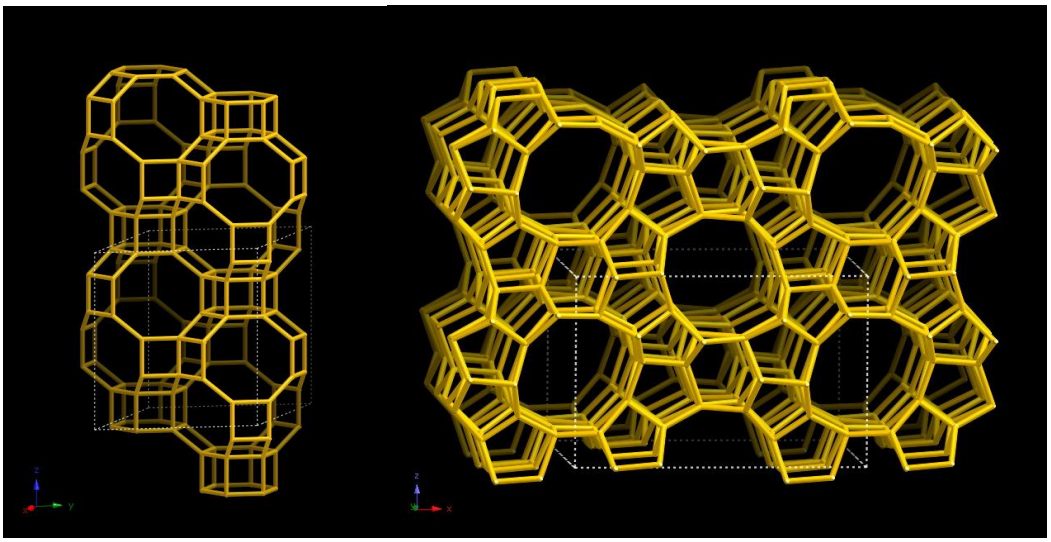

Figure 1: The Framework of SSZ-13 (left image) and ZSM-5 (right image) [13,14]

2.3 DCMM Over Copper Exchanged Zeolites

The exact nature of the active site for DCMM in copper exchanged zeolites is currently under debate [6,8]. An examination of Cu-ZSM-5 initially reported a bis(μ-oxo)dicopper as the active site as revealed by a UV/Vis signal at 22 700 cm^{-1} [6,8]. Examination using Raman spectroscopy pointed towards mono-(μ-oxo)dicopper sites being the active site [6,9]. Then when Cu-MOR catalysts were examined with UV/Vis results pointed towards μ-oxo dicopper sites as being the active species [6,8]. Theoretical calculations indicate that even more types of active in both ZSM-5 and MOR based copper catalysts may exist [6,8]. The difficulty to pinpoint what the active site is, or what they are, makes it difficult to optimize the catalysts. The issue is made more complex by the fact that different zeolites appear to have different, or more diverse types of active sites [8].

The DCMM reaction in copper exchanged zeolites is a quasicatalytical, stepwise reaction cycle. The cycle is composed of an activation, a reaction and an extraction step. The activation stage is typically always performed at high temperatures above 450°C [8]. The oxidizing agent is usually oxygen,

although other compounds may be used, for example nitrogen oxide. Different oxidants may lower the temperature required for activation depending on the zeolite [8]. At the reaction step methane is introduced to the system, often diluted. As the methane adsorbs on the active sites it forms methoxy groups. The partial pressure of methane in the system at this stage influences yield, with higher pressure producing higher yields [9]. The effect of increasing the pressure varies depending on the zeolite, while it increases the yield the effect is not always proportional to the increase in pressure [8]. The methoxy groups formed on the active sites are strongly absorbed, necessitating extraction using a solvent, typically water. The extraction step also deactivates the catalyst [6,8]. The stepwise reaction cycle can be repeated, as hydrated copper species are more readily oxidized this can lead to higher yields [8].

3. Experimental Methods

These sections provide the theoretical background to the experimental procedures that were conducted in this thesis.

3.1 Sample Preparation

The H-ZSM-5 zeolite had been bought and the H-SSZ-13 zeolite had been synthesized in a previous study. Additionally, the H-ZSM-5 sample was functionalized with copper and only required application to a monolithic structure. The H-SSZ-13 sample however, required functionalization with copper salt. Two monoliths wash coated with H-SSZ-13 and H-ZSM-5 had also been prepared in a previous experiment and were utilized in this thesis.

3.1.1 Aqueous Ion Exchange

The H-SSZ-13 zeolite was functionalized with copper using aqueous ion exchange. The zeolite is dissolved into solvent with the desired ion. The desired ions will then diffuse into the zeolite structure and replace the ions already bonded onto the zeolite structure. The replaced ions will then diffuse out of the zeolite structure [15,16,17]. Ion exchange is an equilibrium reaction, once the equilibrium has been reached the zeolite is filtered, washed and calcined. Fixating the ions on the zeolite structure [15,16,17].

6.9764 g of $Cu(NO_3)_2$ salt (produced by Sigma Aldrich, 98%) was measured and dissolved in 300 ml of Milli-Q water. The solutions' pH was 5. 3.0019 g of H-SSZ-13 was added gradually under stirring. The suspension was then stirred for 24 hours, then filtered and dried at 120^{o}C for 23h. The yield was 2.6271g of Cu-SSZ-13.

3.1.2 Wash Coating

Two monoliths were wash coated with Cu-SSZ-13 and two with Cu-ZSM-5. The monoliths, figure 2, had 69, 1 mm by 1 mm wide square channels. The length of the monoliths was 14 mm.

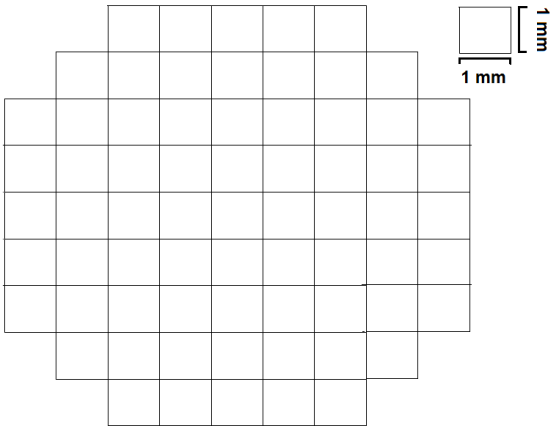

Figure 2: Sketch of the monolithic structure used. Each channel is 1 mm by 1 mm wide.

The desired weight for the wash coat is 0.2 g per monolith. 0.32 g of the powder sample was dissolved with 0.08 g of P2 Disperal binding material in Milli-Q water. The monoliths were then dipped several times into the slurry, with excess suspension removed by an air flow. Following each dipping step, the monolith was dried for five minutes under 90°C followed by a two minutes calcination step at 550°C. The wash coated monoliths were then calcined for one hour at 500°C. The oven was heated at a rate of 5°C/min, from room temperature, to 500°C. Table 1 displays the resulting weight of each sample.

Table 1: Displays the weight for each wash coat and the weight of the catalytic material.

Material	Catalyst + binder weight (g)	Wash coat weight (g)	Catalyst weight (g)
Cu-SSZ-13 (1)	0,3223 + 0,07922	0,2092	0,1679
Cu-SSZ-13 (2)	0,6422 + 0,1606	0,1880	0,1504
Cu-ZSM-5 (1)	0,3219 + 0,0809	0,1935	0,1546
Cu-ZSM-5 (2)	0,3287 + 0,084	0,1960	0,1561

3.2 Nitrogen Physisorption - BET

Nitrogen physisorption is performed in order to evaluate surface area and pore volume of the sample. The calculations for surface area are performed using the BET (Brunauer-Emmet-Teller) theory. Nitrogen molecules, or other non-polar molecules, are physiosorbed on the sample during constant temperatures at varying pressures. The BET theory is a simplification of physisorption based on the Langmuir theory [18,19]. Several assumptions must be made while using the BET theory. These assumptions all concern how a specie adsorbs and subsequent behavior while adsorbed [18,19,20]. Depending on the sample these assumptions introduce an error. This thesis is utilizing zeolites which are porous materials. It is reasonable to expect some errors based on the nature of pore filling versus the assumption of how mono- and multilayers are formed [18,19].

Nitrogen physisorption was used to determine the surface area and pore volume of the Cu-SSZ-13 sample. The Cu-ZSM-5, H-ZSM-5 and H-SSZ-13 samples were measured in a previous study. The results are presented in this thesis as a comparison.

The Cu-SSZ-13 sample with a wet weight of 0,1821g was placed inside a dried quartz tube and was degassed for approximately 4 hours under a nitrogen gas flow at 200°C. Surface area measurements were then started. Dry weight of the sample is 0,1557g. Tests were carried out under -195,8°C. The N_2-sorption was carried out in a TriStar 3000 produced by Micrometrics.

3.3 X-Ray Diffraction - XRD

Powder X-ray diffraction (XRD) provides information about crystal structure and size of a material. In XRD an X-ray source sends radiation at a rotating powder sample, which diffracts the radiation. Diffracted, or reflected, radiation is detected by a detector opposite to the radiation source. Detected radiation has followed Bragg's Law, equation 1. Where *n* is an integer, *d* is the distance between crystal planes, θ is the angle between the plane and the incoming radiation and λ is the wavelength of the radiation [21].

$$n\lambda = 2d * sin(\theta), n=1, 2, 3... \quad \text{eq. 1}$$

XRD was performed for the Cu-SSZ-13 sample. H-SSZ-13, Cu- and H-ZSM-5 and Cu/SiO_2 were measured in a previous study. The diffraction spectra of these samples are presented as comparisons. A diffraction spectrum also existed for a previously created Cu-SSZ-13 sample, which is also presented as a comparison.

The Cu-SSZ-13 sample was placed in a sample holder and positioned in the X-ray diffractometer. The angle changed from 20° to 66° in steps of 0.029° in the experiment and the radiation was produced using a copper anode. The Diffractometer was of the D8 ADVANCE model by Bruker.

3.4 Mass Spectrometry

Mass spectrometry separates compounds on a mass to charge ratio. As what is being analyzed needs to carry a charge the analyte is subject to ionization. There are multiple ionization techniques to achieve this, which vary depending on system setup and type of analyte. In general, ionization techniques can be divided into two groups, hard and soft. Where hard ionization techniques provide high fragmentation and soft provides generally intact molecules [22]. The mass spectrometer in this thesis achieved hard ionization through electron impact. The ions are then accelerated into the mass analyzer section by a repeller or a magnetic field. The strength of the magnetic field in the mass analyzer is what separates the ions. If the ion does not have a mass to charge ratio that lies within the set interval of the mass analyzer, they will not hit the detector. The strength of the magnetic field can vary over a scan to allow for detection of multiple ions [22].

Mass spectrometry was used to monitor the composition of the outflow from DRFITS. The model was an HPR-20 QIC Benchtop Gas Analysis by Hiden Analytical.

3.5 Infrared Spectroscopy

Infrared (IR) spectroscopy utilizes light from the infrared spectrum (λ= 2.5 μm - 25 μm) to excite molecules. The adsorption energy of IR radiation corresponds to energy changes in the molecules of about 8-40 kJ/mole and this energy increases the amplitude of stretching and bending of covalent

bonds [22]. IR spectroscopy can therefore be said to identify molecules per their types of covalent bonds.

Due to each covalent bond having a unique natural frequency of vibration, which is made further distinct by the extended environment the involved atoms find themselves in, it is possible to discern between two molecules with the same composition, yet different structures. Molecules exhibiting symmetry and a lack of dipolar moments are however undetectable by IR, as the radiation cannot be absorbed by such molecules. Even if the radiation frequencies are correct [22].

FT-IR collects data in the time-domain spectrum. The data collected needs to be mathematically processed by Fourier transformation to the frequency-domain and analyzed. FT-IR uses a wide range of infrared light at once by producing an interferogram. The interferogram is a combined beam of different path lengths produced by an interferometer [22]. Which is a setup of a beam splitter and mirrors [22]. The interferogram is directed towards the sample and the modified radiation is measured. As the interferogram contains all the energy from the radiation source at varying wavelengths. The modified interferogram, after having passed the sample, contains information about absorption at every frequency. This transmitted interferogram is then compared to that of a laser, as a reference. After Fourier transformation, the data can be read as a spectrum [22]. To measure a compound, it is typical to also take a spectrum of the background. The background spectra are then subtracted from any measurement.

IR spectroscopy was used to qualitatively and quantitatively measure the outflow from the flow reactor experiments. The IR spectrometer was of the model Multigas 2030 FTIR by MKS Instruments for the flow reactor experiments.

3.5.1 Diffuse Reflectance Infrared Fourier-Transform Spectroscopy

Diffuse Reflectance FT-IR Spectroscopy (DRIFTS) is employed to analyze bound surface species. Surface bound species does not exhibit rotational transitions, the spectra of a bound molecule is therefore different from the same molecule's spectra in the gas phase [23]. As the molecule is adsorbed, the spectra also provide information on what the molecule is adsorbed to. Since the environment is different. DRIFTS can penetrate a short distance into the sample, it is however hard to discern how deep it penetrates. As it varies depending on the sample [23].

DRIFTS was used to analyze bound surface species while running protocol 6 and 7 for Cu-ZSM-5 and Cu-SSZ-13 powder samples. DRIFT was performed using a Vertex 70 by Bruker. It was coupled with a mass spectrometer of the model HPR-20 QIC Benchtop Gas Analysis by Hiden Analytical used to measure the composition of the outflow.

3.6 Flow Reactor

The flow reactor is constructed to perform selectivity and activity testing of catalysts. It allows for control of temperature, feed composition and flow rate in the system.

A schematic over the flow reactor can be seen in figure 3. The gas composition of the inflow was controlled by several mass flow controllers (MFC). Each MFC controlled the flow of one of the gases used. The MFC were in turn controlled by a program stating the flow rates. The outflow from the flow

reactor went to the FT-IR and the exhaust. The temperature in the reactor and the catalysts were measured by two separate thermocouples.

The monolith sample was placed inside a quartz tube, in the middle of two blank monoliths. The blank monoliths were to ensure a good gas flow through the sample. For the same reason the monolith facing the inflow was wrapped in quartz wool. The thermocouple measuring the catalyst temperature was positioned through the center of the monoliths, ending roughly in the sample monolith's middle section. The thermocouple measuring the reactor temperature was positioned was arbitrarily. With the condition that it ended in the middle section of the furthest-most blank monolith from the outflow. The quartz tube is wrapped in a heating coil. The quartz tube and housings for in- and outflow were wrapped in fiberglass for insulation. The reactor setup is horizontal with the inflow placed to the right, when facing the device.

All MFC models were produced by Bronkhorst High-tech. The FT-IR model was a HPR-20 QIC Benchtop Gas Analysis produced by Hiden Analytical.

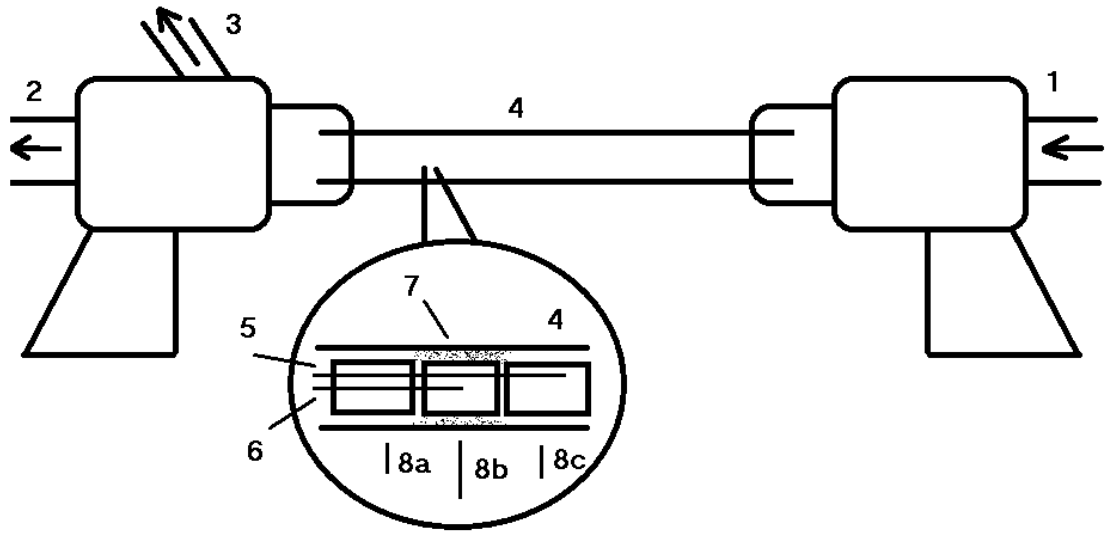

Figure 3: Schematic of the reactor setup. 1) Inflow, 2) Outflow, 3) Thermocouple connections, 4) Quartz tube, 5) Thermocouple 1 - Reactor temperature, 6) Thermocouple 2 - Catalyst temperature, 7) Quartz Wool, 8) Monoliths a) Blank 1, b) Sample, c) Blank 2. The heating coil and fiberglass insulation is not depicted.

3.6.1 Reaction Conditions

In this thesis various reaction conditions were tested. Figure 4, 5 and 6 details the various temperature profiles along with gases used. The flow rate was 1000 ml/min when oxygen, ammonia and hydrogen was flowing. 500 ml/min when methane was flowing and 300 ml/min while water was.

Protocol 1 is denoted as the standard reaction conditions in this thesis. Protocol 2 is an extraction study, to examine if lower water temperatures can be effective at extracting methanol. Protocols 3 to 5 are activation studies under different temperatures. These protocols utilize a mix of oxygen and ammonia (NH_3) for the activation step following a reduction step using hydrogen. The reduction step

is performed as the previous steps using oxygen also activates the catalysts, in addition to cleaning them. Protocols 6 and 7 are also activation studies using NH_3. Unlike protocol 3 to 5 these protocols do not utilize hydrogen in a reduction step and do not feed NH_3 and O_2 in the same step.

The idea behind using ammonia stems from the use of copper exchanged zeolites in NO_x SCR catalysis. The ammonia adsorbs on copper, forming $(Cu\text{-}NH_3)_4$ complexes [24]. These complexes are gaseous and not bound to the zeolite structure. It is theorized that these complexes can diffuse through the zeolite structure and in doing so disperse the copper ions [25,26]. Given the fact that the reactive sites for methane conversion are not fully understood, it is unclear if this will improve the activity of the catalyst or not.

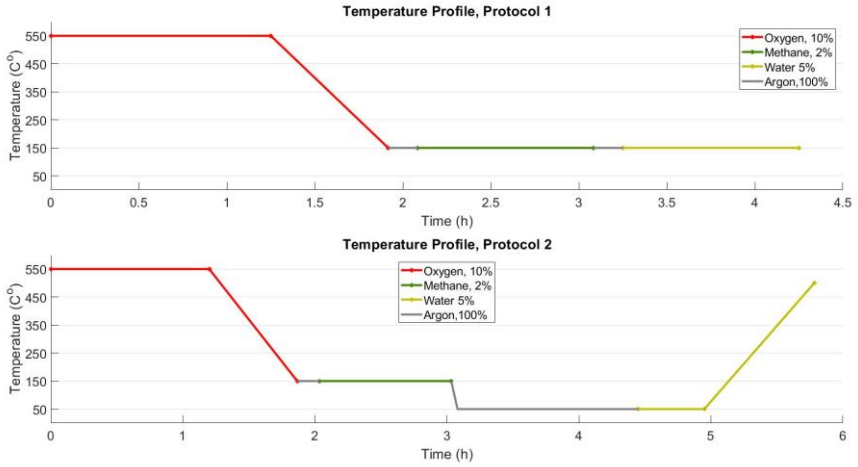

Figure 4: Protocol 1 and 2. The legend denotes the composition of the gas flows; argon was used as a carrier gas.

.

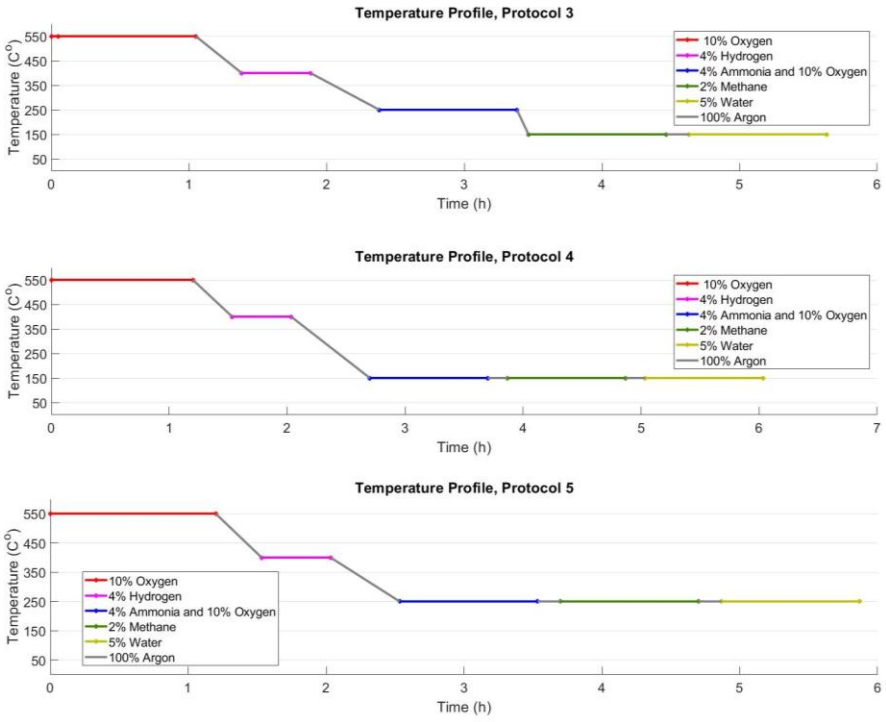

Figure 5: Protocols 3 to 5 with NH_3. The legend denotes the composition of the gas flows, argon was used as a carrier gas.

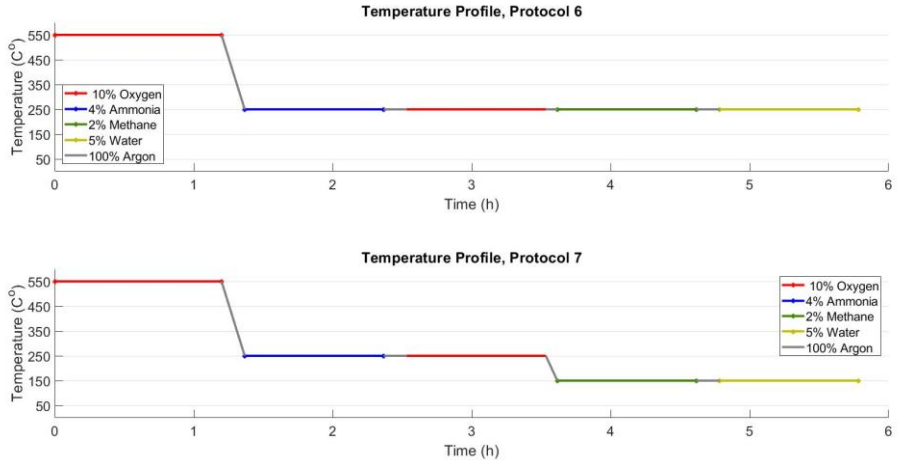

Figure 6: Protocol 6 and 7 with NH_3. Unlike protocol 3-5 the NH3 and O2 flow separately. The legend denotes the composition of the gas flows, argon was used as a carrier gas.

4. Results

These section presents the results of the flow reactor experiments, DRIFT sessions, Nitrogen physisorption and XRD. The results are presented along with a short explanation.

4.1 Flow Reactor

After the first session with the flow reactor the Cu-SSZ-13 samples prepared for this study were deemed to be of dubious quality, see section 4.4. The samples were exchanged for another monolith coated with Cu-SSZ-13 prepared during a previous study. All experiments and protocols mentioned using Cu-SSZ-13 denote to this sample, not the one created during this study.

Two sessions were performed with the flow reactor. The first session produced results for all protocols except for protocol 3, 6 and 7. Although only for the copper zeolite samples, Cu-SSZ-13 and Cu-ZSM-5. During the second session all remaining samples and protocols were run. Which are protocols 3, 7 and 8 for the Cu-SSZ-13 and Cu-ZSM-5 samples. Protocols 1 to 8 for the H-SSZ-13 and H-ZSM-5 samples.

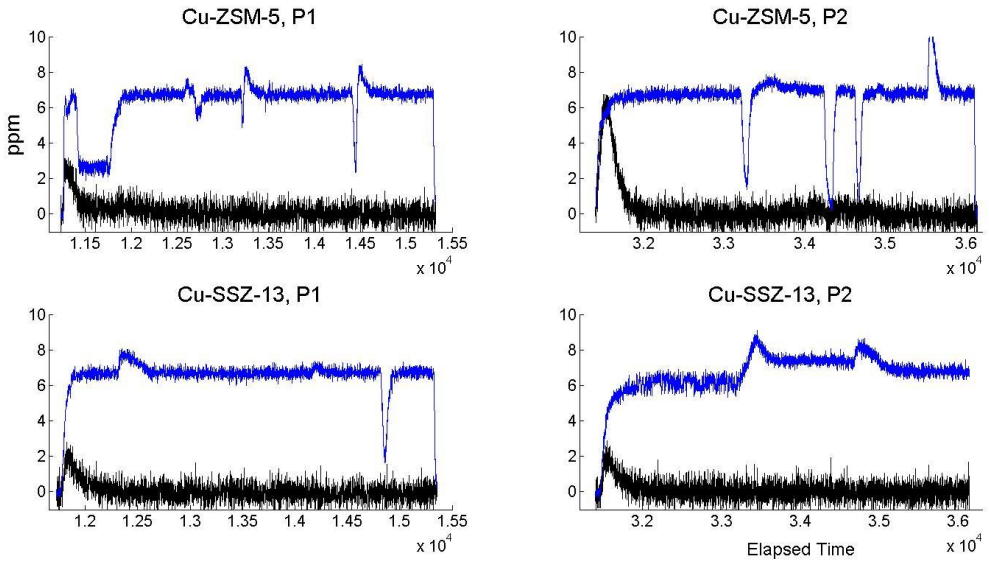

Figure 7: Extraction steps for protocols 1 and 2 for Cu-ZSM-5 (top row) and Cu-SSZ-13 (bottom row). The Y-axis denotes the signal in ppm and the X-axis denotes the time.

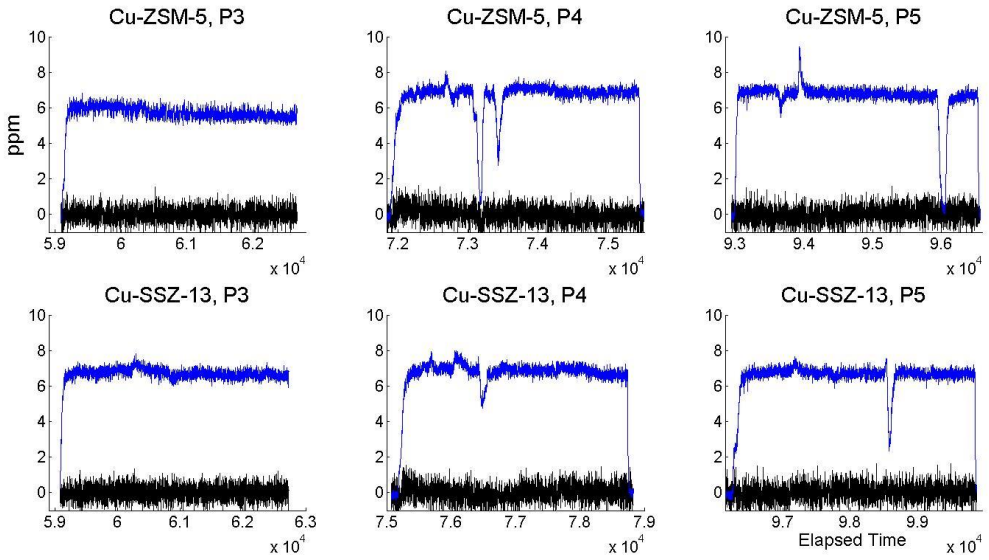

Figure 8: Extraction steps for protocols 3 to 5 for Cu-ZSM-5 (top row) and Cu-SSZ-13 (bottom row). The Y-axis denotes the signal in ppm and the X-axis denotes the time.

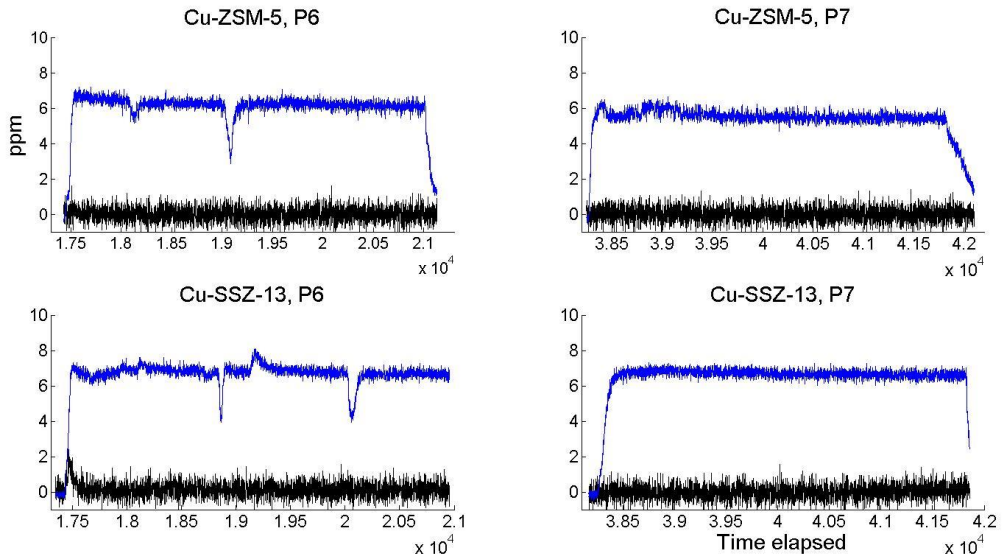

Figure 9: Extraction steps for protocols 6 and 7 for Cu-ZSM-5 (top row) and Cu-SSZ-13 (bottom row). The Y-axis denotes the signal in ppm and the X-axis denotes the time.

The extraction steps of protocols 1 and 2 are shown in figure 7, protocols 3-5 in figure 8 and protocols 6-7 in figure 9. Peaks are visible for the methanol signal in protocol 1 and 2 in figure 7 for both Cu-ZSM-5 and Cu-SSZ-13. As well as protocol 6 for Cu-SSZ-13 in figure 9. The presence of these peaks allows for a qualitative assessment that methanol has been produced. A quantitative assessment of methanol is complicated by signal noise and interference from ammonia. Results are however presented in figure 10.

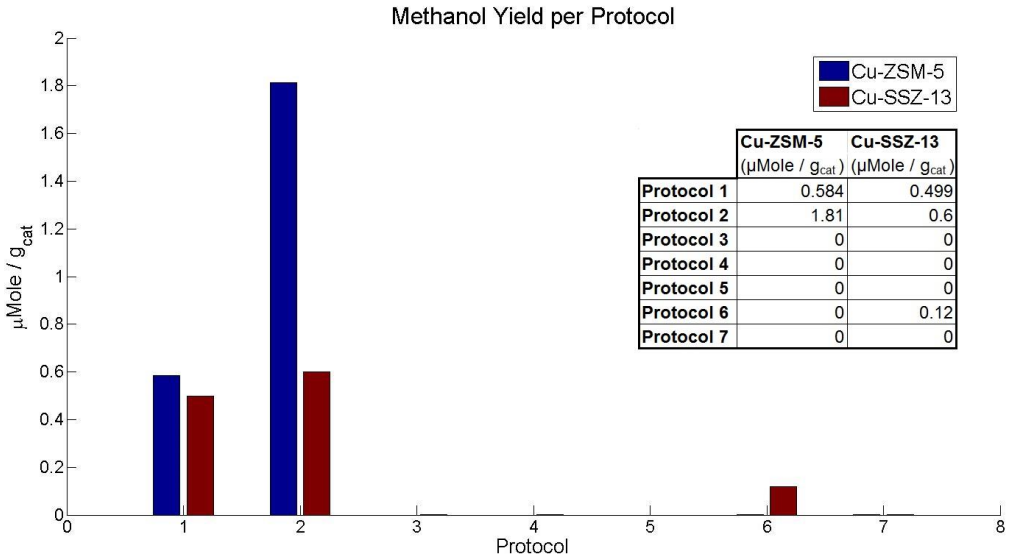

	Cu-ZSM-5 (µMole / g_{cat})	Cu-SSZ-13 (µMole / g_{cat})
Protocol 1	0.584	0.499
Protocol 2	1.81	0.6
Protocol 3	0	0
Protocol 4	0	0
Protocol 5	0	0
Protocol 6	0	0.12
Protocol 7	0	0

Figure 10: Bar chart displaying the methanol yield per gram catalyst for protocols 1-7 for Cu-ZSM-5 and Cu-SSZ-13.

4.2 Diffuse Reflectance Infrared Fourier-Transform Spectroscopy

DRIFTS was conducted on Cu-ZSM-5 and Cu-SSZ-13 powders utilizing modified versions of protocol 6 and 7, see figure 6. Cu-ZSM-5 was not run under protocol 7 due to a lack of time. Each spectrum was taken after the corresponding step in the reaction cycle after the DRIFTS cell was flushed with argon. Background spectra was taken prior to the ammonia step.

Both Cu-ZSM-5 and Cu-SSZ-13 formed copper-ammonia (Cu-$(NH_3)_4$) complexes in protocol 6 as can be seen in figure 12 and 11 respectively. (Cu-$(NH_3)_4$ complexes were also observed for Cu-SSZ-13 in protocol 7, see figure 13. As the (Cu-$(NH_3)_4$ complexes are forming the mobile phase the dispersal of copper is assumed to have been achieved. Methoxy-groups were identified in the Cu-SSZ-13 sample under protocol 6 visible in figure 14. Which is agreeable with the results from the flow reactor experiments, where protocol 6 produced methanol. Neither Cu-ZSM-5 or Cu-SSZ-13 while running protocol 7 displayed any peaks correlating to methoxy-groups. It was not possible to accurately discern what the methoxy groups were bonded on.

Table 2: List of compounds that were of interest and the frequency at which they occur

Compound	**Frequency**	**Reference**
NH_3 adsorbed on Bronsted acid site	3400-3100, 1455-1448, 1409-1393	[24]
NH_3 adsorbed on Cu	3400-3100, 1619, 1278	[24]
NH_3 adsorbed on EFAl	1620, 1332-1324	[24]
Methoxy bonded on...		
Extra framework Si (asym)	2957	[27]
Extra framework Si (sym)	2854	[27]
Extra framework Al	2968	[27]
Brønsted acid site (asym)	2978, 3064, 3148	[27]
Brønsted acid site (sym)	2867, 2968	[27]
Cu^+-$O(H)CH_3$	2942, 3024, 3148	[27]
Cu^+-OCH_3	2792, 2829, 2882	[27]
Cu^{2+}-OCH_3	2693, 2930, 2984	[27]
Cu^+-$O(H)CH_3$-Cu^+	2971, 3080, 3095	[27]
Cu^+-OCH_3-Cu^+	2903, 2987, 3016	[27]
Methanol…		[27]
Hydrogen bonded	2849, 2955, 3002	[27]
Hydrogen bonded, Brønsted acid site	2841, 2909,2991, 3056	[27]

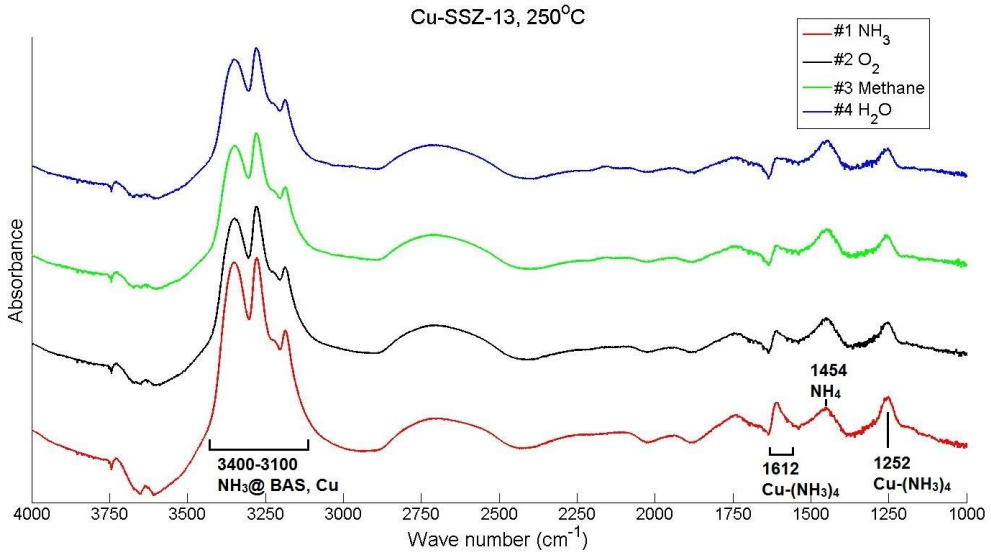

Figure 11: DRIFTS spectra of Cu-SSZ-13 while running protocol 6. See table 2 for reference peaks.

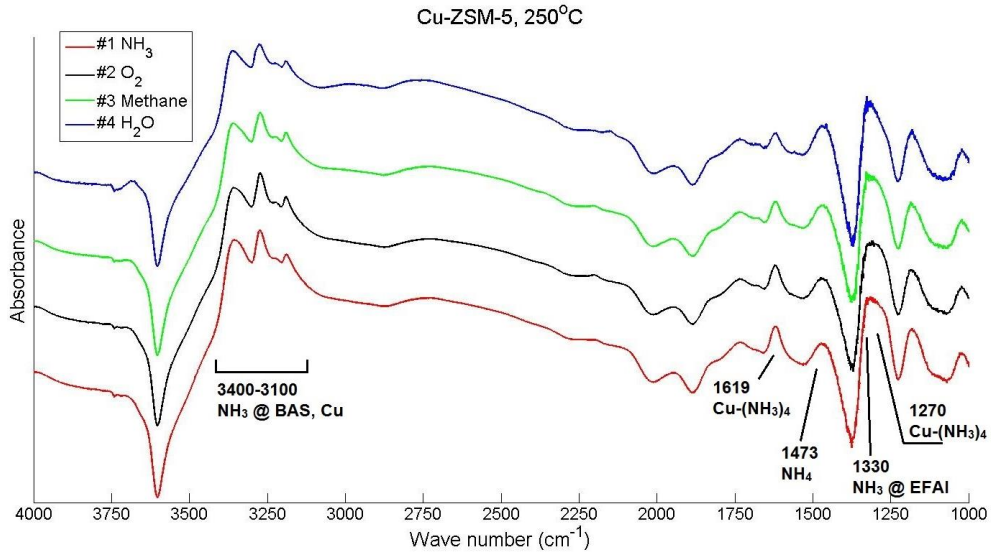

Figure 12: DRIFTS spectra of Cu-ZSM-5 while running protocol 6. See table 2 for reference peaks.

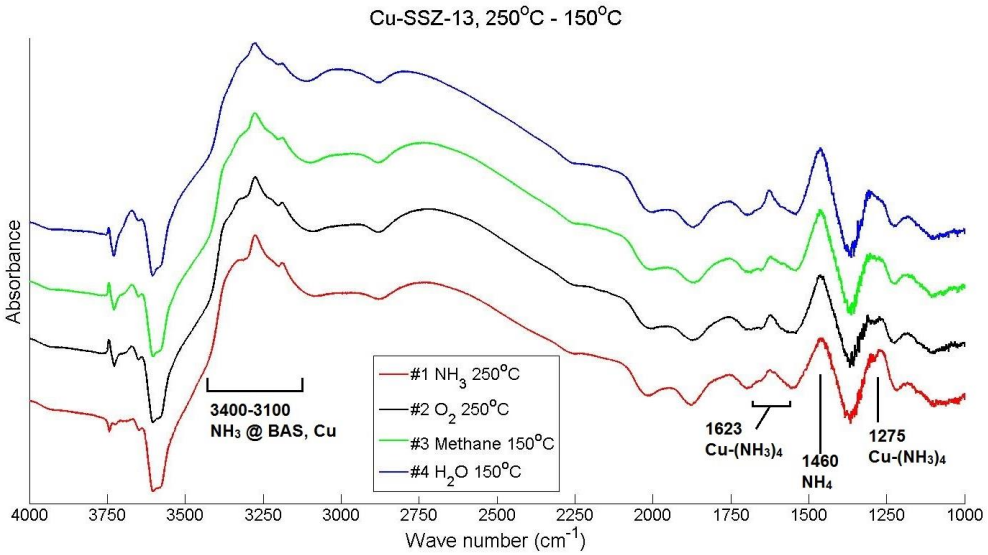

Figure 13: DRIFTS spectra of Cu-SSZ-13 while running protocol 7. See table 2 for reference peaks.

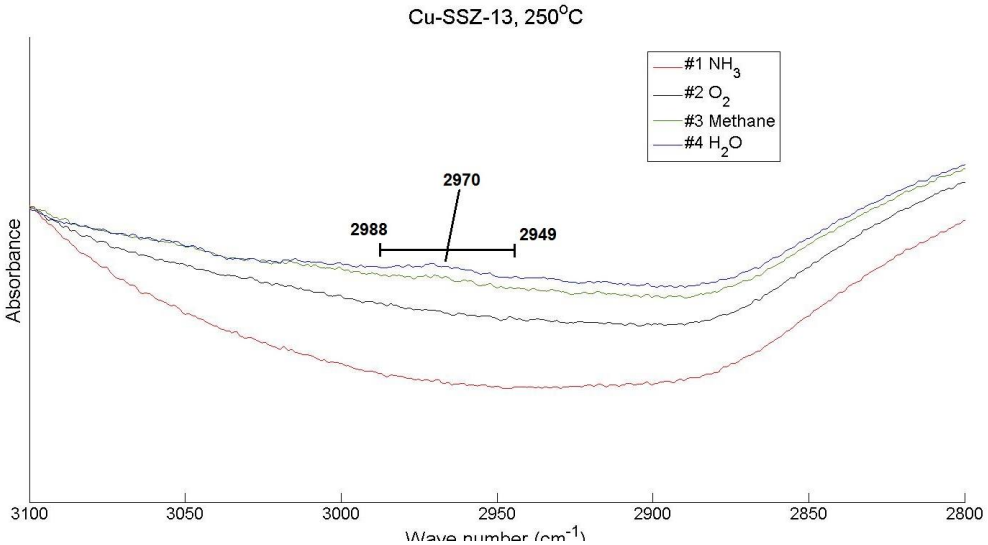

Figure 14: DRIFTS spectra of Cu-SSZ-13 while running protocol 6.

4.3 Nitrogen Physisorption - BET

The surface area and pore volume of the materials used in this thesis are displayed in table 3. The ZSM-5 zeolite shows a loss of surface area when functionalized with copper. This appears not to be the case for the SSZ-13 zeolite, however the XRD results in section 4.4 display that the functionalized SSZ-13 has smaller particles. As such any eventual loss in surface area for Cu-SSZ-13 may be offset by the larger surface area provided by smaller particles. No BET data was provided for the replacement Cu-SSZ-13 sample. The loss of surface area for the functionalized ZSM-5 sample may be due to deposited copper in the structure.

Table 3: Surface area and pore volume of the SSZ-13 and ZSM-5 samples.

Zeolite	Surface Area (m^2/g)	Pore Volume (cm^3/g)
H-ZSM-5	357.23 ± 9.31	0.1048
Cu-ZSM-5	326.70 ± 7.65	0.1127
H-SSZ-13	657.42 ± 15.79	0.1926
Cu-SSZ-13	736.65 ± 22.29	0.2076

4.4 XRD

The Cu-SSZ-13 sample prepared in this study was the only sample to be examined in this thesis. As can be seen in figure 15 the intensity is low, which indicates small particles. Compared to the previously prepared Cu-SSZ-13 sample in figure 16, the difference in intensity is substantial. The peaks align with the H-SSZ-13 sample, also seen in figure 16, and it can thus be stated that the sample is indeed SSZ-13.

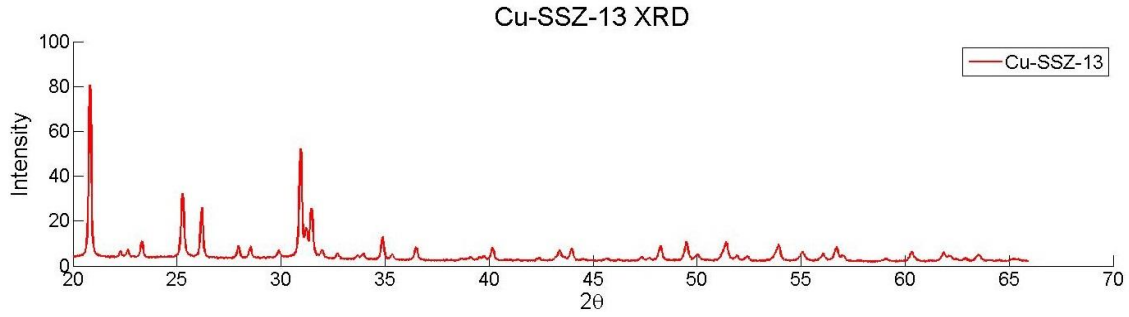

Figure 15: Diffraction spectra for the Cu-SSZ-13 sample prepared in this study.

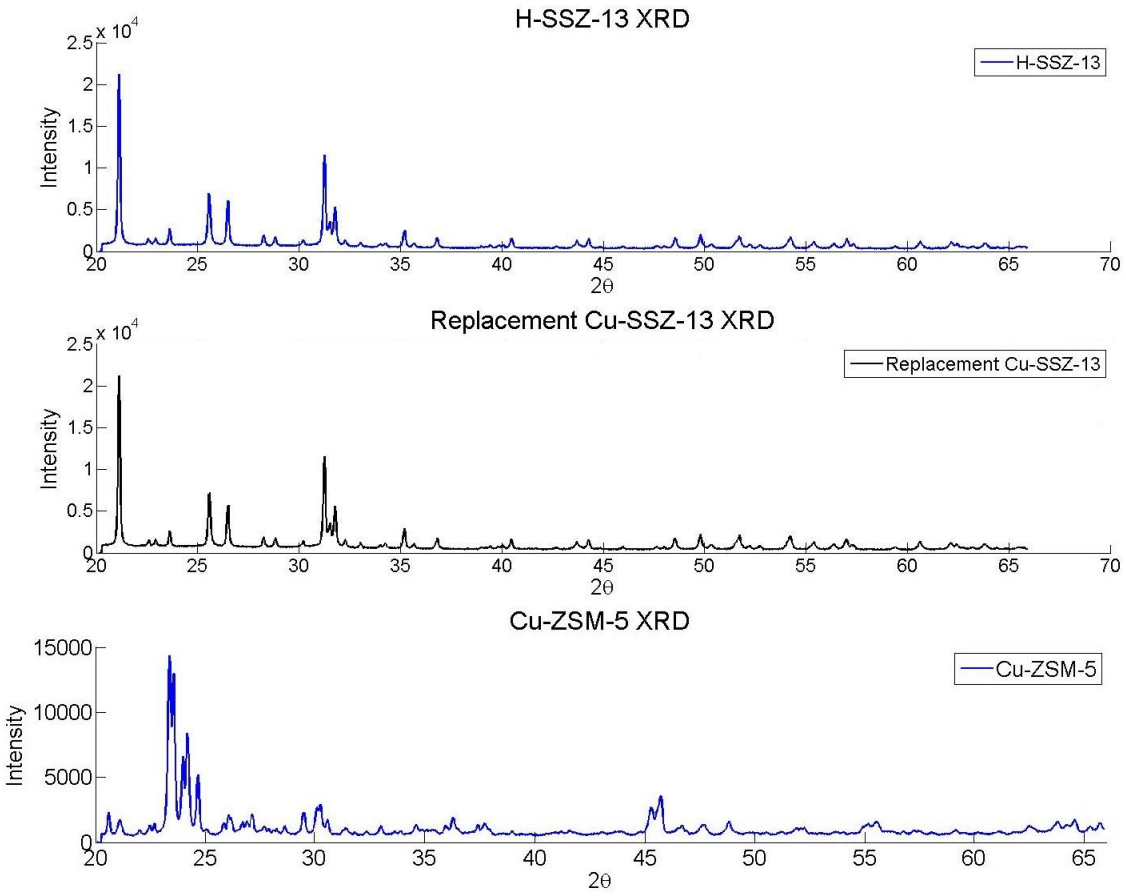

Figure 16: Diffraction spectra for the borrowed Cu-SSZ-13, Cu-ZSM-5 and H-SSZ-13 samples measured in a previous study

Copper cannot be identified in the samples, comparing the diffraction pattern of H-SSZ-13 in figure 16 to that of Cu-SSZ-13 figure 15 and 16 reveal no additional peaks. It is however reasonable to assume that copper is present, both from the flow reactor results and the ion exchange procedure, in which the sample changed colour. As such, any copper in the sample must reside at a depth deeper than 3 nm, which is how far the X-rays penetrate the sample. The Cu-ZSM-5 sample in figure 16 was compared to a theoretically calculated spectrum. The powder pattern was generated from the IZA tool provided at the organization's webpage.

5. Discussion

Of the seven reaction conditions used in this thesis only two, protocol 1 and 2, yielded methanol for all samples. Protocol 6 yielded methanol for Cu-SSZ-13, although at a smaller amount than either protocol 1 or 2 for the same sample.

There exists a difference in yield between the extraction study of protocol 2 and the standard reaction condition (SRC), protocol 1. As can be observed in Figure 5, the Cu-ZSM-5 sample has a substantially larger methanol peak during the low temperature extraction than for the SRC extraction. Cu-SSZ-13 exhibit the same phenomena but to a lesser degree. The difference in yield for Cu-ZSM-5 is nearly three times the amount of methanol, while it is roughly 20% for Cu-SSZ-13. The increased yield can be due to several reasons.

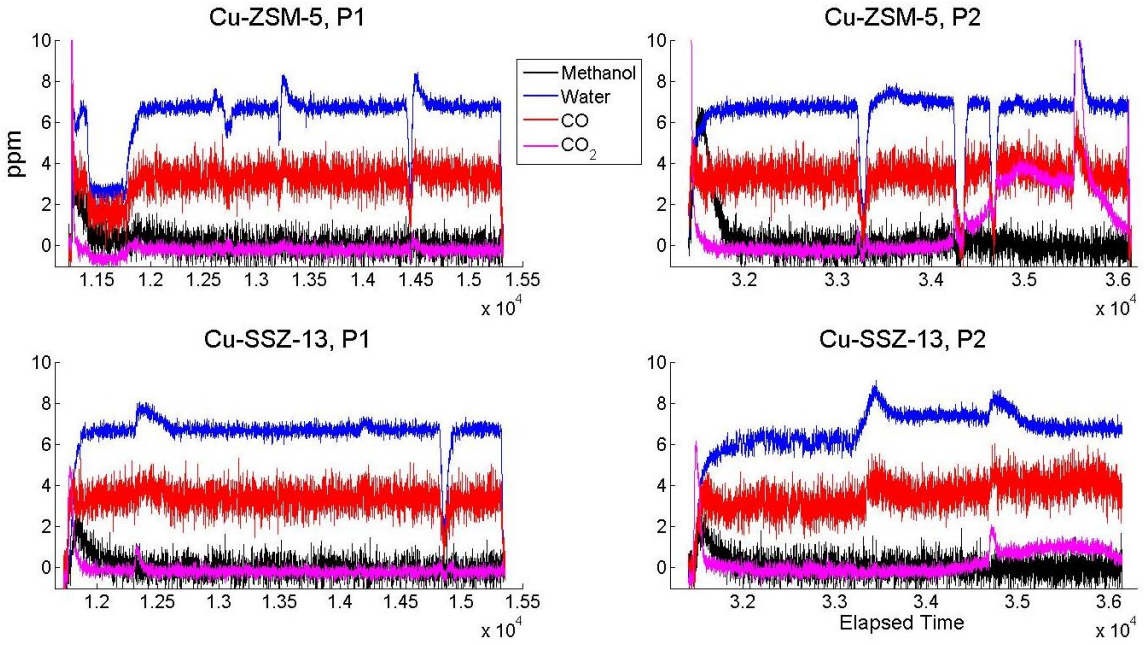

Figure 17: The extraction steps of protocol 1 and 2 for Cu-ZSM-5 and Cu-SSZ-13. With CO and CO2 concentration in addition to methanol and water.

The extraction may simply be more efficient at a lower temperature. This could mean that not all the methoxy is desorbed from the surface at standard reaction conditions. The methanol may also oxidize further at a higher temperature extraction. Figure 16 displays the extraction steps for protocol 1 and 2 with both copper exchanged zeolites. Unlike figure 5 this figure includes the carbon monoxide and dioxide signals. Both the CO_2 and CO signals remain constant in both protocols and samples until the temperature increases in protocol 2. Protocol 2 appears to produce relatively less CO_2 than protocol 1 for Cu-ZSM-5. However, Cu-SSZ-13 displays the opposite behavior, with an increase in the CO_2 signal relative that of the methanol.

As mentioned in section 2.3, hydrated copper species are more readily oxidized. Which leads to increasing yields as the reaction cycle is repeated. While running the protocols in the flow reactor they were run back to back. Protocol 1 was run first of all the protocols and prior to protocol 2. There was no rest period in between the extraction step of protocol 1 and the oxidation step of protocol 2. How this would affect the results were not considered, neither is it known how large this influence is. It is likely that this increased the yield of protocol 2 compared to protocol 1, but it may not completely account for it.

Nevertheless, the selectivity for methanol and the conversion of methane have increased for Cu-ZSM-5 under low temperature extraction. If indeed the lower extraction temperature is responsible for either requires further trials. Cu-SSZ-13 also appear to have increased conversion of methane, but the selectivity towards methanol is lower. As the temperature of extraction increases so does the CO_2 and CO signals, this may indicate that not all the methoxy is extracted, or that some other carbohydrate is present on the sample. Extraction is however viable at 50°C.

The activation studies using ammonia did not produce methanol, except for protocol 6. Which only did so for the Cu-SSZ-13 sample and had the lowest yield of any methanol producing protocol. Protocol 6 share temperature profile with protocol 4, the difference between the protocols is the flow

composition, see figures 5 and 6. While no protocol flowing ammonia and oxygen in a conjoined step was examined using DRIFT, it was assumed that no oxidation occurred in these protocols. Ammonia is reductive and the oxidation temperature is low, the oxidized copper may have been deactivated in these steps. The independent ammonia and oxygen flows of protocol 6 may have provided some activation. Not on par with the regular activation at 550ºC however. Yet the ammonia and oxygen steps in protocol 7 occur under the same conditions as in protocol 6 and no methanol was produced. It is possible that the reaction temperature is also a factor as no methoxy groups were visible. Verification of copper oxides in the DRIFT spectra would have provided more answers as to which step is failing.

It can be concluded that ammonia does not reduce the temperature of activation under the majority of tested conditions. It would have benefited this thesis if a protocol similar to protocol 1 had been tested, with oxidation performed at 250ºC. To be used as a comparison to protocol 6, or indeed any of the activation studies. If no oxidation is possible at this temperature without the influence of ammonia, it may warrant further investigation. That Cu-SSZ-13 yielded results while Cu-ZSM-5 did not may could also warrant investigation into how other copper exchanged zeolites perform under these conditions.

It was possible from the DRIFT spectra to discern that copper-ammonia complexes formed. It appeared that, in the case of the one successful experiment, this may have allowed for activation of Cu-SSZ-13 at a temperature of 250ºC. No reduction step using hydrogen was performed in protocol 6, so it is possible that the initial oxidation was responsible for the activated sites, not the oxidation step at 250ºC. It is not possible to draw any conclusions as to the dispersal of copper in the zeolites. As no copper oxide peaks could be identified. It could be worthwhile to examine and adequately quantify the effect of the dispersal with some other method than DRIFTS.

6. Conclusions

The low temperature extraction is viable. Whether or not low temperature extraction yields more methanol or increases selectivity is something that must be examined further. The difference in effect between the two catalysts is also interesting. It could indicate that the copper either disperses differently on the two zeolites or that the active sites are somehow different.

Ammonia does not appear to lower the activation energy of copper exchanged ZSM-5 or SSZ-13. The similarities between the activation studies that did not produce methanol and the one that did points to more factors being at play.

7. References

[1] Faramawy, S & Zaki, Tamer & Sakr, Ayat. (2016). Natural gas origin, composition, and processing: A review. Journal of Natural Gas Science and Engineering. 34. 10.1016/j.jngse.2016.06.030.
[2] BP Statistical Review of World Energy, June 2018. Retrieved 2019-02-11 https://www.bp.com/content/dam/bp/business-sites/en/global/corporate/pdfs/energy-economics/statistical-review/bp-stats-review-2018-full-report.pdf
[3] United Nations Climate Change, Global warming potentials. Retrived 2019-02-05 https://unfccc.int/process/transparency-and-reporting/greenhouse-gas-data/greenhouse-gas-data-unfccc/global-warming-potentials
[4] Emam, E.A. (2015) Gas Flaring in Industry: An Overview. Petroleum & Coal, 57, 532-555.
[5] Natural Gas Flaring, Processing, and Transportation, Union of concerned Scientists, Retrieved 2019-02-11 https://www.ucsusa.org/clean-energy/coal-and-other-fossil-fuels/natural-gas-flaring-processing-transportation#.XGF9c1VK71
[6] The Direct Catalytic Oxidation of Methane to Methanol - A Critical Assessment
M. Ravi, M. Ranocchiari, J. A. van Bokhoven, *Angew. Chem. Int. Ed.* 2017, *56*, 16464.
[7] Iron and Copper Active Sites in Zeolites and Their Correlation to Metalloenzymes
Benjamin E. R. Snyder, Max L. Bols, Robert A. Schoonheydt, Bert F. Sels, and Edward I. Solomon
Chemical Reviews 2018 *118* (5), 2718-2768, DOI: 10.1021/acs.chemrev.7b00344
[8] Direct Conversion of Methane to Methanol under Mild Conditions over Cu-Zeolites and beyond
Patrick Tomkins, Marco Ranocchiari, and Jeroen A. van Bokhoven
Accounts of Chemical Research 2017 *50* (2), 418-425, DOI: 10.1021/acs.accounts.6b00534
[9] Catalytic Oxidation of Methane into Methanol over Copper-Exchanged Zeolites with Oxygen at Low Temperature, Karthik Narsimhan, Kenta Iyoki, Kimberly Dinh, and Yuriy Román-Leshkov, ACS Central Science 2016 *2* (6), 424-429, DOI: 10.1021/acscentsci.6b00139
[10] Scott M. Auerbach, Kathleen A. Carrado, Prabir K. Dutta, *Handbook of Zeolite Science and Technology*. Marcel Dekker, Inc. New York
[11] Database of Zeolite Structures, International Zeolite Association. Framework type MFI. Retrieved 2019-04-18. http://europe.iza-structure.org/IZA-SC/framework.php?STC=MFI
[12] Database of Zeolite Structures, International Zeolite Association. Framework type CHA. Retrieved 2019-04-19. http://europe.iza-structure.org/IZA-SC/framework.php?STC=CHA
[13] Database of Zeolite Structures, International Zeolite Association. Image of MFI structure. Retrieved 2019-04-22
http://europe.iza-structure.org/IZA-SC/framework_main_image.php?STC=CHA
[14] Database of Zeolite Structures, International Zeolite Association. Image of CHA structure. Retrieved 2019-04-22
http://europe.iza-structure.org/IZA-SC/framework_main_image.php?STC=MFI
[15] Männikkö, Marika & Skoglundh, Magnus & Härelind, Hanna. (2012). Selective catalytic reduction of NOx with methanol over supported silver catalysts. Applied Catalysis B: Environmental. 119. 256-266. 10.1016/j.apcatb.2012.03.006.
[16] Ertl G (1999), *Preparation of Solid Catalysts*, Wiley-VCH, Weinham
[17] Inglezakis, V.J & Poulopoulos, S.G, *Adsorption, Ion Exchange and Catalysis*, Elseveir 2006
[18] Adsorption of Gases in Multimolecular Layers, Stephen Brunauer, P. H. Emmett, and Edward Teller
Journal of the American Chemical Society **1938** *60* (2), 309-319, DOI: 10.1021/ja01269a023
[19] Kenneth Sing, The use of nitrogen adsorption for the characterisation of porous materials,
Colloids and Surfaces A: Physicochemical and Engineering Aspects, Volumes 187–188, 2001, Pages 3-9, ISSN 0927-7757, https://doi.org/10.1016/S0927-7757(01)00612-4.

[20] Verification of the BET-theory by experimental investigations on the heat of adsorption. Johannesson, Björn. Division of Building Materials, LTH, Lund University, 2000. 58 p. (Report TVBM; Vol. 3096).
[21] C. Suryanarayana, M. Grant Norton, *X-Ray Diffraction: A Practical Approach*, Springer Science+Business Media, LLC

[22] Pavia, Lampman, Kriz, Vyvyan, *Introduction to Spectroscopy 5th Edition*. Cengage Learning, Bellingham Washington
[23] Niemantsverdriet JW (2000), *Spectroscopy in Catalysis, Second Edition*. Wiley-VCH Verlag GmbH, Weinheim
[24] Determining the storage, availability and reactivity of NH_3 within Cu-Chabazite-based Ammonia Selective Catalytic Reduction systems, I. Lezcano-Gonzalez, U. Deka, B. Arstad, A. Van Yperen-De Deyne, K. Hemelsoet, M. Waroquier, V. Van Speybroeck, B.M. Weckhuysen, A.M. Beale. *Phys. Chem. Chem. Phys.*, 2014,16, 1639-1650, DOI:10.1039/C3CP54132K
[25] Dissociation of ammonia on a copper surface and the effect of oxygen coadsorption: a quantum-chemical study, G.J.C.S. van de Kerkhof W.Biemolt, A.P.J.Jansen, R.A.van Santen
Surface Science, Volume 284, Issue 3, 20 March 1993, Pages 361-371
[26] Narsimhan K, Iyoki K, Dinh K, Román-Leshkov Y. Catalytic Oxidation of Methane into Methanol over Copper-Exchanged Zeolites with Oxygen at Low Temperature. *ACS Cent Sci*. 2016;2(6):424–429. doi:10.1021/acscentsci.6b00139
[27] Methanol Desorption from Cu-ZSM-5 Studied by In Situ Infrared Spectroscopy and First-Principles Calculations. Xueting Wang, Adam A. Arvidsson, Magdalena O. Cichocka, Xiaodong Zou, Natalia M. Martin, Johan Nilsson, Stefan Carlson, Johan Gustafson, Magnus Skoglundh, Anders Hellman, and Per-Anders Carlsson. The Journal of Physical Chemistry C 2017 *121* (49), 27389-27398, DOI: 10.1021/acs.jpcc.7b07067